

SLAC-PUB-4875
February 1989
(I)

DEVELOPMENT OF CRID SINGLE ELECTRON WIRE DETECTOR*

D. ASTON^a, A. BEAN^c, T. BIENZA^a, F. BIRD^{a1}, D. CALDWELL^c, M. CAVALLI-SFORZA^d, P. COYLE^d, D. COYNE^d, S. DASU^a, W. DUNWOODIE^a, G. HALLEWELL^a, K. HASEGAWA^g, J. HUBER^c, P. JACQUES^f, R. A. JOHNSON^c, H. KAWAHARA^a, Y. KWON^a, D. LEITH^a, A. LU^c, J. MARTINEZ^e, L. MATHYS^c, S. MCHUGH^c, B. MEADOWS^e, M. NUSSBAUM^e, R. MORRISON^c, R. PLANO^f, B. RATCLIFF^a, P. RENSING^a, D. SCHULTZ^a, S. SHAPIRO^a, A. SHOUP^e, C. SIMOPOULOS^a, E. SOLODOV^{a2}, P. STAMER^f, I. STOCKDALE^e, N. TOGE^a, J. VA'VRA^{a3}, D. A. WILLIAMS^d, S. WILLIAMS^a, M. WITHERELL^c, R. J. WILSON^b, J. S. WHITAKER^b, S. YELLIN^c, H. YUTA^g

^aStanford Linear Accelerator Center, Stanford University, Stanford, CA 94309

^bBoston University, Department of Physics, Boston, MA 02215

^cUniversity of California, Department of Physics, Santa Barbara, CA 93106

^dSanta Cruz Institute for Particle Physics, University of California,
Santa Cruz, CA 95064

^eUniversity of Cincinnati, Department of Physics, Cincinnati, OH 45221

^fRutgers University, Department of Physics, New Brunswick, NJ 08903

^gTohoku University, Department of Physics, Aramaki, Sendai 980, Japan

Abstract

We describe the R&D effort to define the design parameters, method of construction and experimental results from the single electron wire detectors. These detectors will be used for particle identification using the Čerenkov Ring Imaging techniques in the SLD experiment at SLAC. We present measurements of pulse heights for several gases as a function of gas gain, charge division performance on a single electron signal using both 7 μm and 33 μm diameter carbon wires, photon feedback in TMAE laden gas, average pulse shape, and its comparison with the predicted shape and cross-talk. In addition, we present results of wire aging tests, and other tests associated with construction of this unusual type of wire chamber.

* Work supported by the Department of Energy, contracts DE-AC03-76SF00515 and DE-AT03-79ER70023, and by the National Science Foundation under grants PHY85-12145 and PHY85-13808.

¹ Present Address: EP Division, CERN, CH1211, Geneva 23, Switzerland.

² Permanent Address: Institute of Nuclear Physics, Novosibirsk, 630090, USSR.

³ Speaker.

Presented by J. Va'vra at the International Wire Chamber Conference,
Vienna, February 13-17, 1989.

1. Introduction

A Čerenkov detector must have a high efficiency for detecting single photoelectrons. Our detector measures the axial coordinate of the photoelectron along the drift box axis by measuring the drift time, the radial coordinate along the drift box depth by measuring the charge division on each wire, and the azimuthal coordinate by the wire address. The radial coordinate is essential for the reduction of the parallax broadening on the Čerenkov ring images. The use of TMAE (tetrakis-dimethylamino ethylene), which serves as a photocathode, strongly influences the detector design parameters, such as a photon feedback, the wire aging, etc. A review of the overall CRID system is presented in an accompanying paper at this Conference [1].

2. Detector description

Each of the 40 barrel CRID single electron detectors will be instrumented with 93 anode wires of 10.35 cm length and on a 3.175 mm pitch. The suppression of photon feedback is realized by the geometry shown in fig. 1. The walls of the "U" shaped cathode eliminate "direct communication" between neighboring wires. The cathode is made of a nickel-plated, machined aluminum block. Five layers of etched copper-beryllium sheets (blinds) [2], each 254 μm thick, are stacked above the cathode and limit the angle ($\sim 6.6^\circ$) over which photons from the avalanche can reach the drift volume. To ensure flatness, the Cu-Be material is heat treated before etching. In addition, the individual strips are tied together by a 305 μm wide connecting strip in the middle of the chamber. To prevent possible corona discharge on the etched edges, the Cu-Be sheets are electropolished after etching. Before the first blind, there is a wire plane (100 μm Cu-Be wires) which guides the drifting electrons into the openings in the blinds. In addition, this wire plane can also serve as a gate to prevent positive ions from reaching the drift volume and photoelectrons from reaching the anode. This is accomplished by pulsing of the odd and even gate wires by ± 350 V.

To achieve the desired 1% (or 1 mm) position resolution using the charge division technique on single electron signals, it is necessary to reduce the Johnson noise originating in the anode wire. This drives the choice to a 7 μm diameter carbon wire of 40 $\text{k}\Omega$ resistance. To prove the feasibility of using such a wire, a number of tests had to be performed [3]. Many of these results are listed in table 1; here we mention only a few. For instance, it is not easy to establish perfect electrical contact to a carbon wire. We have tried a number of methods, most of them based on various kinds of conducting epoxies. The final choice was a silver based epoxy, H20-E, made by Epotek. In all methods, one develops a residual contact resistivity, which seems to plateau after a certain period of

time—see fig. 2. Uncertainty of $100\ \Omega$ in the contact resistance creates an apparent 0.25 mm coordinate error at the end of the wire.

We also found that wire aging in gases doped with TMAE is much more rapid than in usual drift chamber gases [3, 4]. Figure 3 shows the result of such aging after a dose of about 6 mC/cm , and after the chamber has been opened to air. Before exposure to air, the wire is covered with a smooth film, believed to be electrically nonconductive. This film is responsible for the gain loss. For example, one measures a 50% gain loss after a dose of about 0.2 mC/cm in $\text{C}_2\text{H}_6 + \text{TMAE}$ (27°C) using the $7\ \mu\text{m}$ diameter carbon wire. If one uses a larger wire diameter ($33\ \mu\text{m}$) or a larger carrier gas molecule (like C_4H_{10}), the aging effects are reduced [3,4]. However, it was also discovered that sending a small current of about 11 mA through the wire causes resistive heating to an estimated temperature of 380°C . At this temperature, the wire deposits evaporate, and the wire regains its full efficiency. Of course, the cathodic aging effects are not helped by this method. We are planning to have the wire heating capability in the SLD experiment, although it is to be used as a last resort. Finally, stretching a large number of $7\ \mu\text{m}$ carbon wires requires a careful procedure [3]. It is important to remove weak wires from the sample. This is accomplished by both measuring the resistance and over-tensioning, each wire by 2 g during the stretching. The tension is measured for each wire using a vibration technique where the wire is vibrated by a flow of N_2 gas in presence of a magnetic field [5].

The detector and amplifier [6] are optimized for single electron detection. However, one will also detect the large dE/dx ionization loss from charged particles. Thus, very large signals, equivalent to up to 1000 primary electrons, will also be observed. To minimize the resulting cross-talk, we have incorporated shielded signal traces between the wire and the amplifier input, and used the largest cathode-to-ground capacitor possible, consistent with prevention of wire breakage by a spark—see table 1. The resulting distant wire-to-wire cross-talk is about 0.2–0.3%, and the nearest neighbor cross-talk is at a 1% level for the 0.3 nF cathode-to-ground decoupling capacitor value. The $33\ \mu\text{m}$ wire allows this value to be increased to $\sim 5\text{ nF}$. This would reduce the cross-talk by almost a factor of 2 [7]. Measurements were made, both with an Fe^{55} source, as well as with a single electron signal. It is also important to minimize the signal-to-ground capacitance to achieve low noise. The measured value of the chamber capacitance is about 15 pF .

Experimental Results

The present paper is based on the testing of three single electron detectors, two with $7\ \mu\text{m}$ diameter anode wires [8], and one with $33\ \mu\text{m}$ wires [9] for comparison. Figure 1 shows the experimental setup [10], which is used for non-TMAE gas testing. The UV light strikes a dense stainless steel cloth and creates an electron

Table 1

Parameter	7 μm dia.	33 μm dia.
Wire length ℓ	10.35 cm	10.35 cm
Wire resistance R_W	40 k Ω	5.2 k Ω
Contact resistance (ave.) R_C	150 Ω	30 Ω
Wire tension	6 g	12 g
Wire breaking tension	10.1 ± 2.1 g	60–70 g
Energy needed to break the wire by a spark	0.8 ± 0.3 mJ	> 300 mJ
Max. decoupling capacitor (cathode to ground)	< 0.3 nF	> 5 nF
Distant neighbor cross-talk	0.2–0.3%	—
Cathode voltage V_C	-1.55 kV	-2.05 kV
Average total wire gain Q_{L+R}^{TOT}	$\sim (5 - 6) \times 10^5$	$\sim 6 \times 10^5$
Cathode surface gradient	1.8 kV/cm	3.3 kV/cm
$\sigma_{z/\ell}$ (C_2H_6 gas) – charge division	0.7 %	1.2 %
Slope = dz (meas.)/ dz (true)	0.98	0.86
σ_{NOISE} (calculated) – rms	1100 el.	2540 el.
σ_{NOISE} (measured) – rms	1150 el.	2180 el.
Signal-to-ground capacitance	15 pF	—

which is then used to study the detector response. We use a triggerable UV light source [11]. The light is focused by a system of three variable apertures and a 10 cm focal length quartz lens. The probability to produce one electron per single UV flash is about 1–5%, depending on the aperture opening.

Figure 4 shows single electron pulse spectra measured in C_2H_6 , CH_4 and 80% $\text{CH}_4 + 20\%$ C_2H_6 gases for two different wire diameters, for various cathode voltages, and as a function of total wire charge Q_{L+R}^{TOT} (the total gain calculation includes a correction for the total drift of positive ions, and includes both left and right channel contributions). The present nominal operating choice is C_2H_6 gas, with 7 μm wire operating with a cathode voltage of -1.55 kV (the presence of TMAE will lower this voltage by 50–100 V).

The single electron pulse shapes were digitized by a LeCroy ICA 2261 digitizer (20 ns binning). Figure 5(a) shows many superimposed pulses normalized at the peak. It is interesting to compare the measured and expected pulse shape $C(t)$, which is assumed to be approximated by a convolution of the amplifier response and the positive ion response.

$$\begin{aligned}
 C(t) &= \int_0^t \left(t' e^{-t'/\tau} \right) \left(\frac{1}{t - t' + t_0} \right) dt' \\
 &= e^{-(t+t_0)/\tau} (t + t_0) \left[\ln(1 + t/t_0) + \sum_{n=1}^{\infty} \left(\frac{t_0}{\tau} \right)^n \frac{1}{n \cdot n!} [(1 + t/t_0)^n - 1] \right] \\
 &\quad - \tau(1 - e^{-t/\tau})
 \end{aligned} \tag{1}$$

The amplifier response was measured by injecting charge via a 1 pF capacitor. The data points Δ in fig. 5(b) shows the resulting average pulse shape. It has been fitted with the expected $t e^{-t/\tau}$, yielding $\tau = 65.0$ ns. The agreement is good in the region up to about 600 ns. Figure 5(b) shows the amplifier response convoluted with the positive ion response, using eq. (1). (The avalanche characteristic time t_0 was calculated to be 0.1 ns for CH₄ gas [7].) One can see that the measured detector pulse shape shown by data points \square agrees well with the theoretical pulse shape, except in the region of the tail. This may be due to a slight undershoot in the calibration pulse. In addition, we have neglected effects such as the signal propagation along the wire according to the telegraph equation, and the propagation through the chamber's strip-line feedthrough.

Finally, the most important measurement is the charge division resolution on a single electron signal. Using fig. 6 as a model, we derived eq. (2) to predict the charge division resolution. There are two terms; one contribution is due to the Johnson thermal noise in the wire and is independent of avalanche position; the other is dependent on the avalanche position, the amplifier noise, and the wire end termination. We approximate the amplifier noise by the FET channel-thermal noise contribution [12].

$$\begin{aligned}
 \left(\frac{\sigma_z}{\ell} \right) &\simeq \sqrt{\left(\frac{\sigma_J}{Q_{L+R}^{VIS}} \right)^2 + \left(\frac{\sigma_{AMP}/\sqrt{2}}{Q_{L+R}^{VIS}} \right)^2 \left[\left(\frac{R_{CH}}{FR_w} \right)^2 + \left(\frac{2z}{\ell} \right)^2 \right]} \\
 \sigma_J &= 2.718 \sqrt{\frac{kT\tau}{2R_{CH}}} \quad \sigma_{AMP} \cong 2.718 \sqrt{\frac{kTR_{EQ}(C_{IN} + C_{CH})^2}{2\tau}} \\
 F &= e^{-2T_G/(R_{CH}C)} \approx 1.0
 \end{aligned} \tag{2}$$

In eq. (2), k is the Boltzmann constant, T is absolute temperature, τ is the amplifier's shaping time (65 ns), R_W is the wire resistance, R_C is the wire contact resistance, r is the amplifier input impedance, $R_{CH} = R_W + 2R_C + 2r$, R_{EQ} is the equivalent noise resistance of the FET (50Ω), C_{IN} is the amplifier input capacitance (10 pF), C_{CH} is the detector capacitance (15 pF), T_G is the integration time (200 ns), Q_{L+R}^{VIS} is the visible average charge ($L + R$) obtained during T_G (typically $2\text{--}3 \times 10^5$ el.), and C is the amplifier decoupling capacitor (10 nF). The F factor in eq. (2) is equal to one for most chambers. Using these constants, we obtain $\sigma_J = 960$ el. (2480) and $\sigma_{AMP} = 530$ el. (530) for the $7 \mu\text{m}$ ($33 \mu\text{m}$) wire. Thus, the second term in eq. (2) is almost negligible, and one expects only a small dependence of the resolution on the position of the avalanche along the wire.

Figure 7(a) is a scatter plot of a sum of the left and right pulse heights against the measured z-coordinate for C_2H_6 gas at cathode voltage of -1.55 kV. Figure 7(b) shows its projection onto the z-axis indicating a charge division resolution $\sigma_{z/\ell} = 0.7\%$ (σ_z is derived from the FWHM estimate, *i.e.*, we neglect the non-Gaussian tails of this distribution).

Figure 8 shows the measured charge division resolution as a function of the pulse height slice, for UV light generated electron pulses, and for pulses injected into the amplifiers with the detector connected. In both cases, the noise contribution due to the amplifier noise, the capacitance, and the wire resistance are included. However, in the first case we also have an extra 0.4% contribution to the resolution due to the $400 \mu\text{m}$ beam size (the light beam spot size and electron diffusion). These are compared to calculations based on eq. (2); the calculation does not include the $400 \mu\text{m}$ beam broadening effect.

Figure 9 shows the charge division resolution integrated over all pulse heights as a function of z coordinate for both types of wires. This result indicates that the resolution doesn't change much along the wire, as predicted by eq. (2). The finite size of the beam helps to explain the discrepancy between the calculation and the measurement of the charge division. We have also measured excellent charge division linearity on both types of wire, indicating good resistance uniformity.

At our nominal operating cathode voltage [-1.45 kV for $\text{C}_2\text{H}_6 + \text{TMAE}$ (28°C)], secondary single electron pulses due to photon emission in the primary avalanche were observed at the 0.5% level.

Conclusions

We have demonstrated that our single electron detector promises to detect the Čerenkov photoelectrons well, and that the charge division technique can indeed be used on single electron signal.

Acknowledgments

We would like to thank all the engineering staff for their invaluable help throughout this project. In particular we would like to thank O. Millican, D. McShurley, G. Oxoby, N. Spencer, H. Shaw, and T. Montagne.

References

- [1] D. Aston *et al.*, *Development and Construction of the SLD Čerenkov Ring Imaging Detector*, contribution to this conference presented by G. Hallewell.
- [2] The blinds are made by PCM Products Inc., Titusville, FL 32780.
- [3] J. Va'vra *et al.*, SLAC-PUB-4432; IEEE Trans. Nucl. Sci., **NS-35** (1988).
- [4] J. Va'vra, IEEE Trans. Nucl. Sci., **NS-34** (1987); SLAC-PUB-4116 (1986); CRID Memo #36 (1987), unpublished.
- [5] R. Stephens, P. Rensing, and J. Va'vra, CRID Memo #39 (1987), unpublished.
- [6] E. Spencer *et al.*, IEEE Trans. Nucl. Sci., **NS-35** (1988); SLAC-PUB-4404 (1987). The amplifier used was the MOSFET preamp PC board prototype (BF992 at front end) followed by a differential receiver (NE5539). The total gain of the system was about 2.4 μ V/electron.
- [7] J. Va'vra, CRID Memo #50 (1989), unpublished.
- [8] The 7 μ m wires are made by Toho Rayon Co., Tokyo, Japan.
- [9] The 33 μ m wires are made by Textron Specialty Material Co., Lowell, MA 01851.
- [10] D. Aston *et al.*, SLAC-PUB-4785; IEEE Trans. Nucl. Sci., **NS-36** (1989).
- [11] The UV Xenon lamp L2435 is made by Hamamatsu Co.; the trigger circuit is made at SLAC; the UV gun delivers about 400 Hz with time jitter of 20 ns.
- [12] C. F. G. Delaney, *Electronics for the Physicist*, (Ellis Horwood Publ., 1980).

FIGURE CAPTIONS

- Fig. 1. The experimental setup to test the single electron detectors using a triggerable UV lamp source to create electrons from a dense steel cloth.
- Fig. 2. Contact resistivity between the carbon wires and the silver conducting epoxy (H2O-E made by EPOTEK) as a function of time.
- Fig. 3. Aging deposits in $\text{CH}_4 + \text{TMAE}$ (27° C) on $7 \mu\text{m}$ diameter carbon wire after several hours in air. The deposits were obtained after a total charge dose of about 6 mC/cm [4].
- Fig. 4. The single electron pulse height spectra measured with $7 \mu\text{m}$ wires in: (a) C_2H_6 . (b) $80\% \text{CH}_4 + 20\% \text{C}_2\text{H}_6$. (c) CH_4 gases as a function of total wire gain Q_{L+R}^{TOT} . (d) The same for $33 \mu\text{m}$ wire in C_2H_6 gas.
- Fig. 5. (a) The average measured single electron pulse shape obtained in CH_4 gas with the prototype amplifier [10]. (b) Comparison of an average measured test pulse shape (Δ) and the calculated amplifier response $te^{(-t/\tau)}$, $\tau = 65 \text{ ns}$ (solid line); and the average single electron measured pulse shape (\square) and its calculated shape (dashed line) using eq. (1).
- Fig. 6. Equivalent model of the charge division.
- Fig. 7. (a) The measured z -resolution plotted against a sum of left and right wire pulse heights in C_2H_6 gas $7 \mu\text{m}$ diameter carbon wires and nominal voltages ($V_c = -1.55 \text{ kV}$). (b) Projection of (a) on the z axis ($\sigma_z/\ell = 0.7\%$).
- Fig. 8. Measured and calculated charge division resolution on a single photoelectron as a function of charge slice as selected by a discriminator window; measured using UV lamp for $7 \mu\text{m}$ (\square) and $33 \mu\text{m}$ (Δ) wires; measured using injected calibration pulses while the detector is connected for $7 \mu\text{m}$ (\blacksquare) and $33 \mu\text{m}$ (\blacktriangle); calculations using eq. (2) (solid line).
- Fig. 9. Measured charge division resolution integrated over all pulse heights on a single photoelectron as a function of z -coordinate along the wire for $7 \mu\text{m}$ (\square) and $33 \mu\text{m}$ (Δ) wires; calculation done using eq. (2), assuming the average visible charge Q_{L+R}^{VIS} of 2.25×10^5 and 2.5×10^5 electrons for both types of wires. Dashed lines include $400 \mu\text{m}$ beam size.

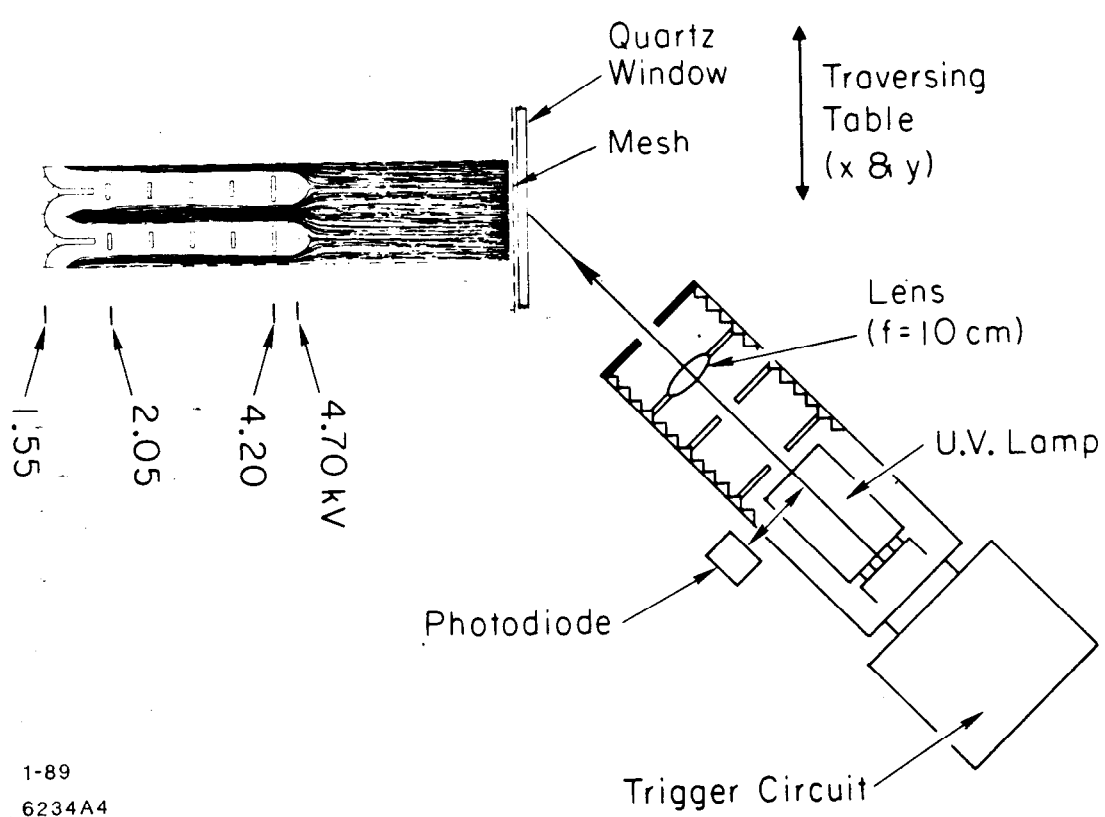


Fig. 1

1-89
6234A4

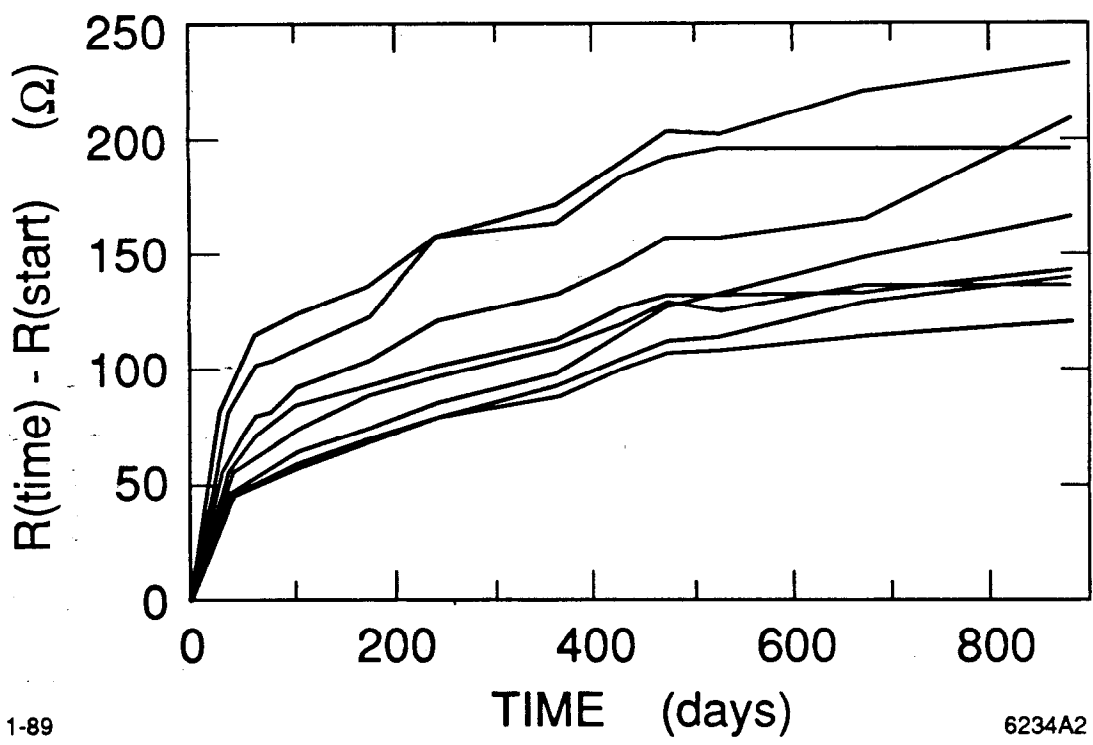


Fig. 2

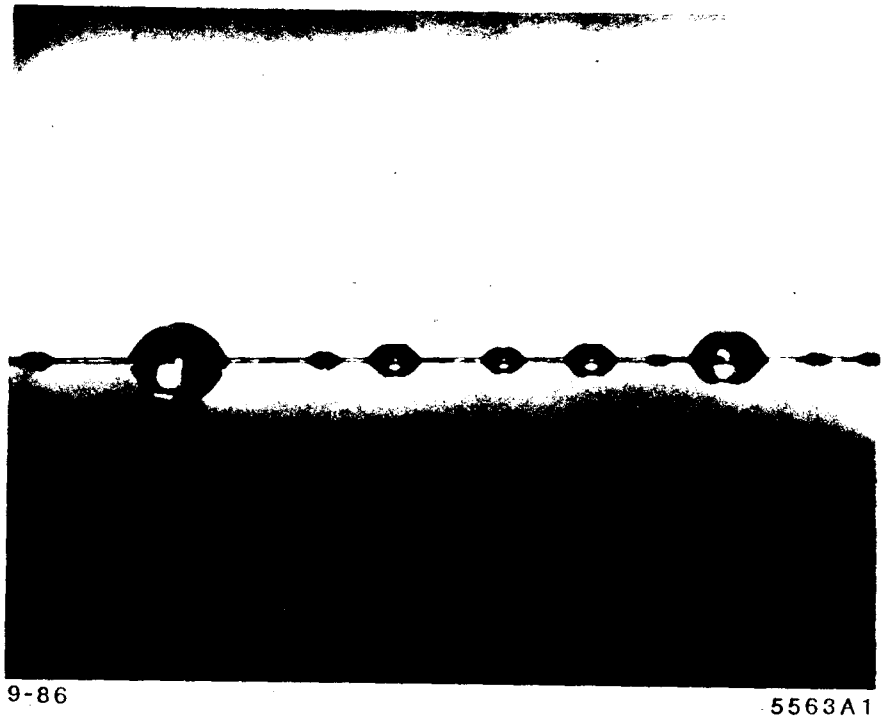


Fig. 3

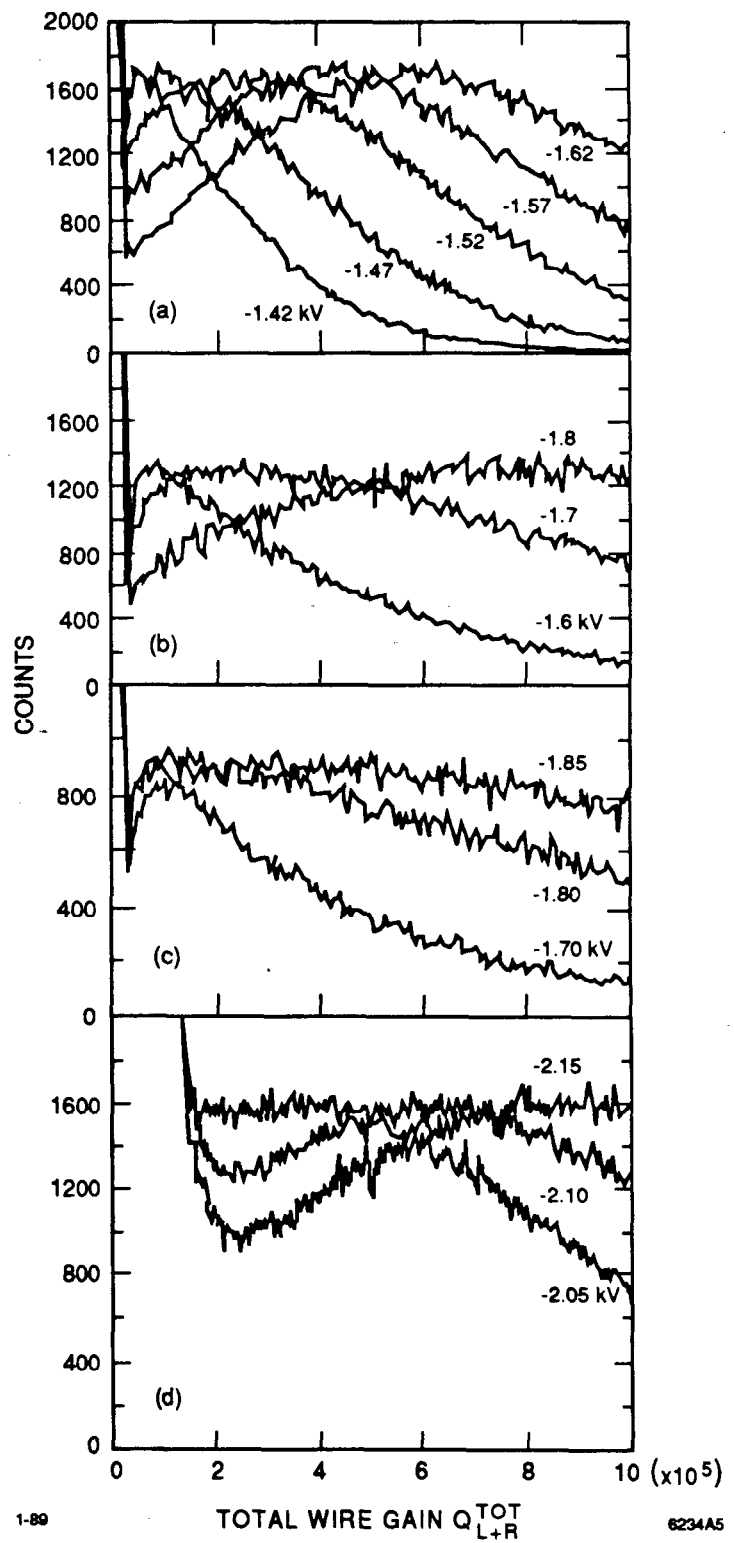
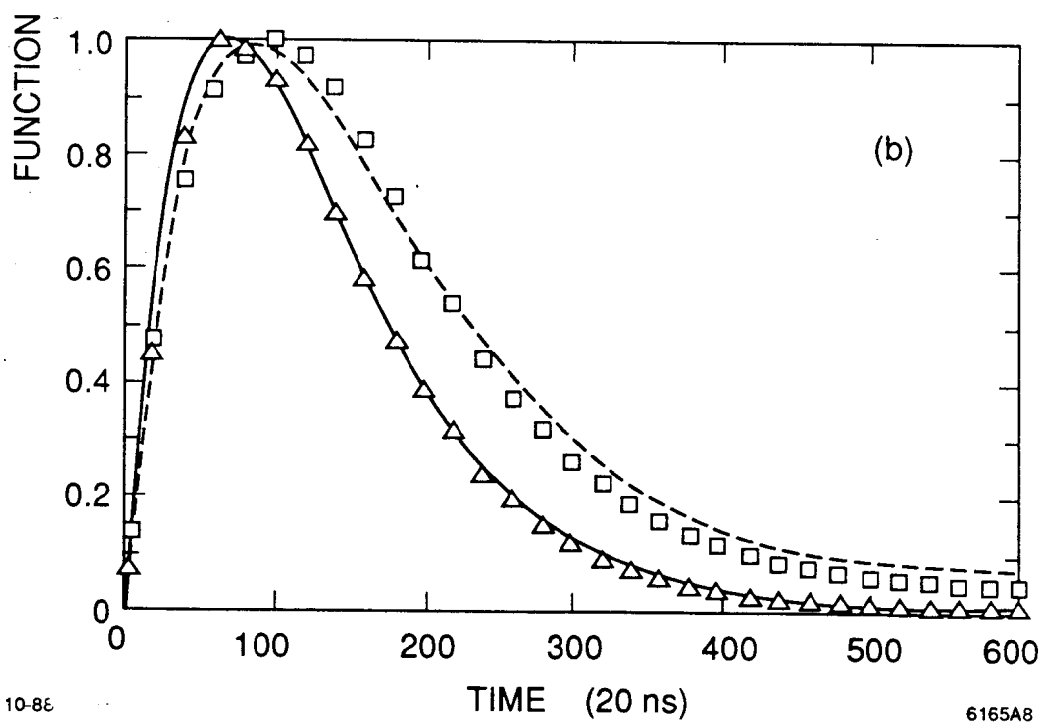
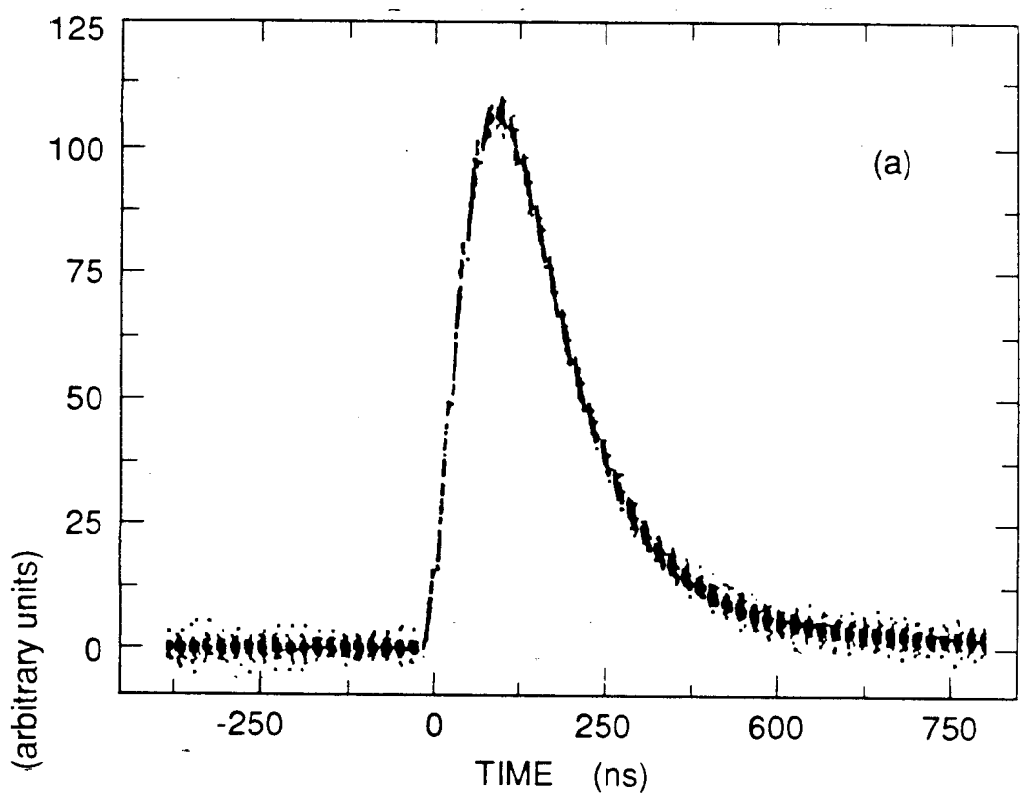


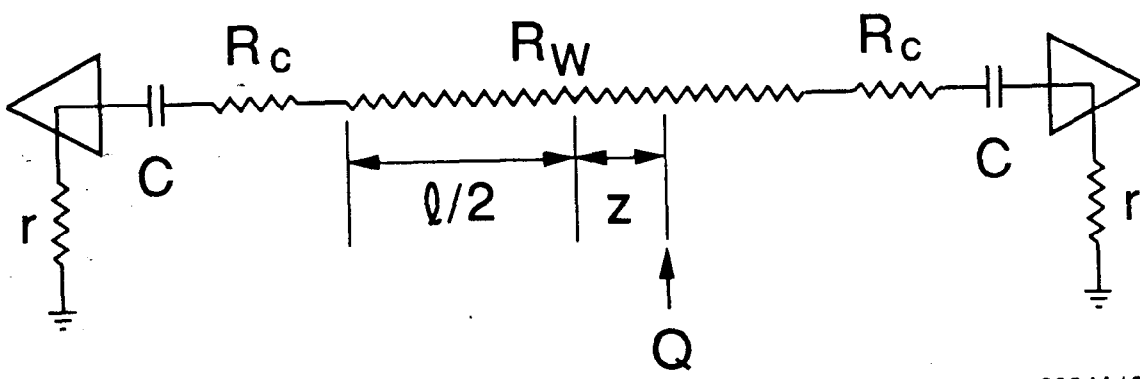
Fig. 4



10-88

6165A8

Fig. 5



1-89

6234A12

Fig. 6

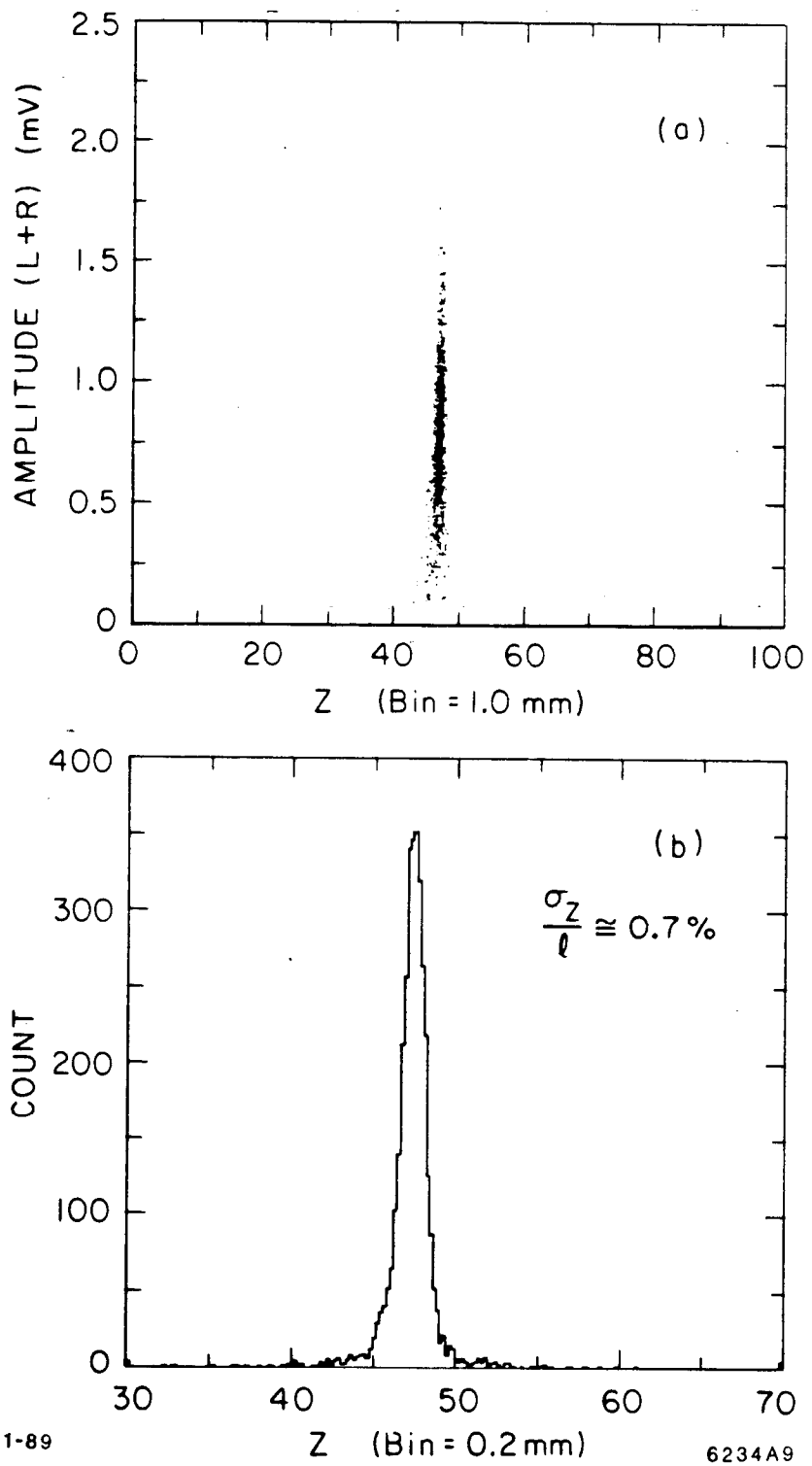


Fig. 7

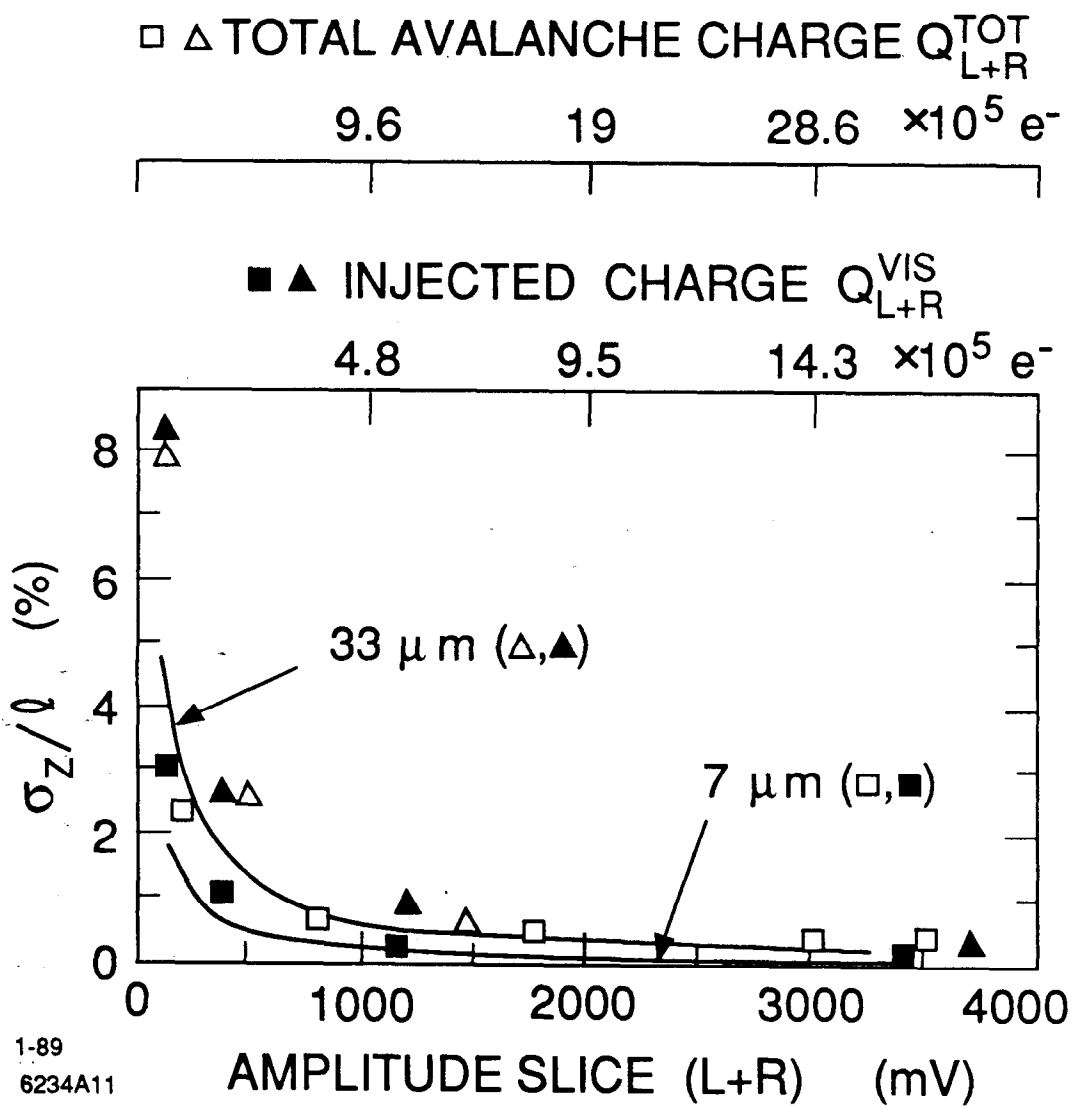


Fig. 8

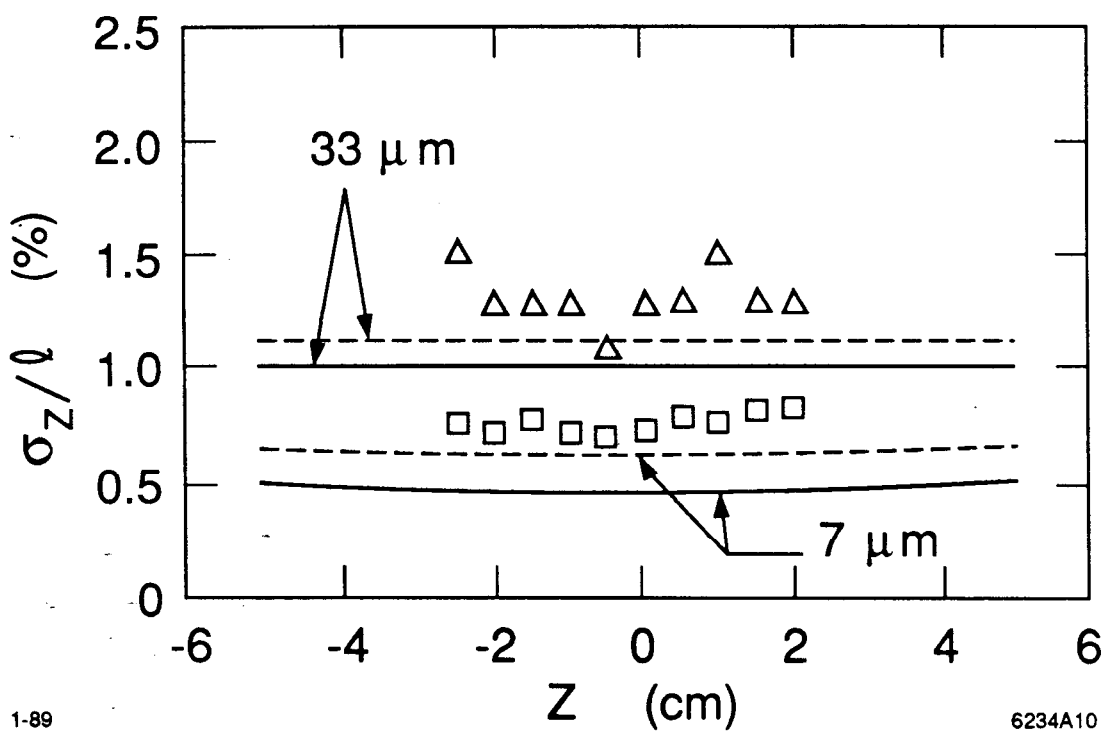


Fig. 9

1-89

6234A10